

Substrate specificity of Rv3378c, an enzyme from *Mycobacterium tuberculosis*, and the inhibitory activity of the bicyclic diterpenoids against macrophage phagocytosis†

Tsutomu Hoshino,* Chiaki Nakano, Takahiro Ootsuka, Yosuke Shinohara and Takashi Hara

Received 15th October 2010, Accepted 14th December 2010

DOI: 10.1039/c0ob00884b

The Rv3378c gene product from *Mycobacterium tuberculosis* encodes a diterpene synthase to produce tuberculosinol (**3**), 13*R*-isotuberculosinol (**4a**), and 13*S*-isotuberculosinol (**4b**) from tuberculosinyl diphosphate (**2**). The product distribution ratios are 1 : 1 for **3** to **4** and 1 : 3 for **4a** to **4b**. The substrate specificity of the Rv3378c-encoded enzyme was examined. The 3 labdadienyl diphosphates, copalyl diphosphate (CDP) (**7**), *ent*-CDP (**8**), and *syn*-CDP (**9**), underwent the conversion reaction, with good yields (67–78%). Copalol (**23**) and manool (**24**) were produced from **7**, *ent*-copalol (**25**) and *ent*-manool (**26**) from **8**, and *syn*-copalol (**27**) and vitexifolin A (**28**) from **9**. The ratio of **23** to **24** was 40 : 27, that of **25**:**26** was 22 : 50, and that of **27**:**28** was 16 : 62. Analysis on a GC-MS chromatograph equipped with a chiral column revealed that **24**, **26**, and **28** consisted of a mixture of 13*R*- (**a**) and 13*S*-stereoisomers (**b**) in the following ratio: *ca.* 1 : 1 for **24a** to **24b**, *ca.* 1 : 5 for **26a** to **26b**, and *ca.* 1 : 19 for **28a** to **28b**. The structures of these products indicate that the reactions of the 3 CDPs proceeded in the same fashion as that of **2**. This is the first report on the enzymatic synthesis of natural diterpenes manool, *ent*-manool, and vitexifolin A. Both Rv3377c and Rv3378c genes are found in virulent *Mycobacterium* species, but not in avirulent species. We found that **3** and **4** inhibited the phagocytosis of opsonized zymosan particles by human macrophage-like cells. Interestingly, the inhibitory activity was synergistically increased by the coexistence of **3** and **4b**. Other labdane-related diterpenes, **13–16** and **23–28**, had little or no inhibitory activity. This synergistic inhibition by **3** and **4** may provide further advantage to the impairment of phagocyte function, which might contribute to pathogenicity of *M. tuberculosis*.

Introduction

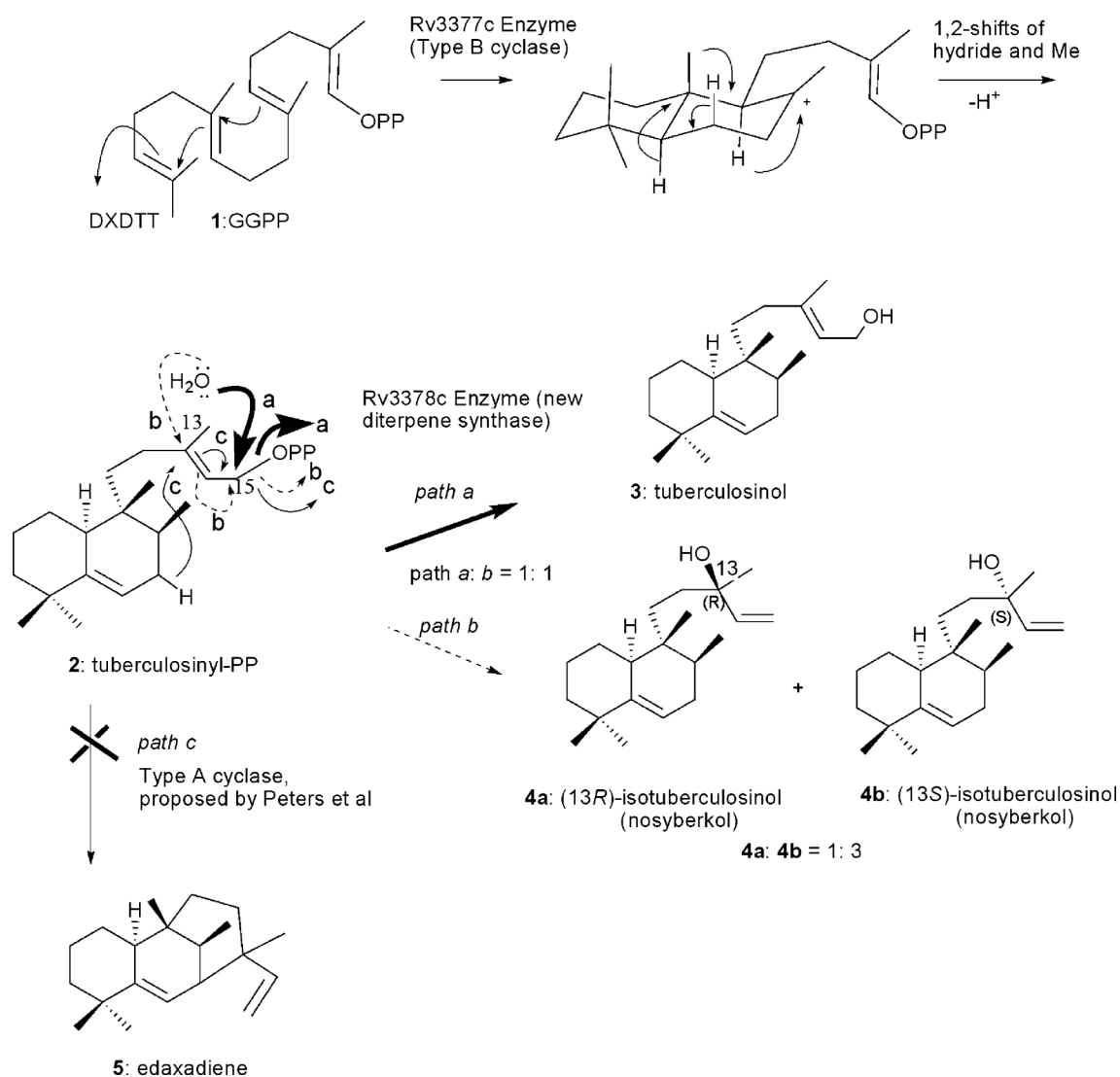
Despite over a century of research, *Mycobacterium tuberculosis* infection is still a leading cause of death worldwide.¹ In previous studies, we have reported the interesting finding that Rv3377c and Rv3378c genes are found in virulent *Mycobacterium* species, but not in avirulent species.^{2–4} The Rv3377c gene product converts geranylgeranyl diphosphate (GGPP, **1**) into tuberculosinyl diphosphate (**2**) with a halimane core.^{2,3,5} Thus, this enzyme is classified as a Type B (Class II) diterpene cyclase. In 2005 and 2006,^{6,7} we presented at research conferences the preliminary result that the flanking gene Rv3378c encodes a diterpene synthase, which afforded both tuberculosinol (**3**) and isotuberculosinol (**4**; alternative name, nosyberkol)⁸ from **2**.⁴ In contrast, in 2009, Peters

and coworkers reported that the Rv3378c enzyme gave **5** as the single enzymatic product, which they named edaxadiene.⁹ They concluded that the Rv3378c enzyme is a Type A (Class I) cyclase. However, the edaxadiene structure of **5** has been revised to **4** by recent chemical syntheses of **4**,^{10,11} which we first proposed as being one of the enzymatic products of Rv3378c.^{6,7} In our previous study,⁴ we have established that the Rv3378c enzyme affords both **3** and **4** in a 1 : 1 ratio and that **4** consists of a mixture of the diastereomers 13*R*-isotuberculosinol (**4a**) and 13*S*-isotuberculosinol (**4b**) in a 1 : 3 ratio.⁴ Thus, this enzyme is a new type of diterpene synthase.⁴ This reaction mechanism is shown in Scheme 1.

Dairi and coworkers isolated the *cyc2* gene from *Kitasatospora griseola*, which encodes the diterpene synthase to afford terpenetriene (**12**) from terpentadienyl diphosphate (**6**).¹² The CYC2 enzyme also accepts acyclic GGPP (**1**) and farnesyl diphosphate (FPP, **10**) as the substrates to produce **17–22**, involving 1,3-butadiene moiety in the structures, but not tolerating geranyl diphosphate (**11**, GPP).¹² Recently, we have demonstrated that the CYC2 enzyme further accepts a variety of bicyclic diterpene diphosphates as the substrate, such as copalyl diphosphate (CDP, **7**), *ent*-copalyl diphosphate

Department of Applied Biological Chemistry, Faculty of Agriculture and Graduate School of Science and Technology, Niigata University, Ikarashi 2-8050, Nishi-ku, Niigata, 950-2181, Japan. E-mail: hoshitsu@agr.niigata-u.ac.jp; Fax: +81-25-262-6854

† Electronic supplementary information (ESI) available: EI-MS and NMR analyses of products **23–28**, inhibitory activities of **3**, **4**, **3+4a** and **3+4b** against macrophage phagocytosis and other data. See DOI: 10.1039/c0ob00884b



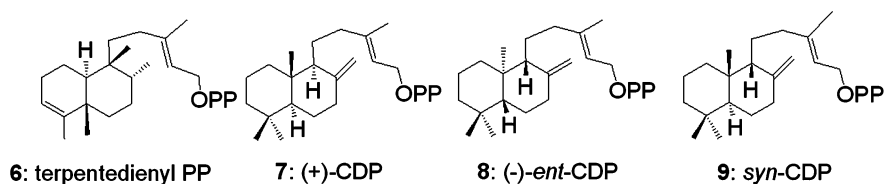
Scheme 1 Chemical mechanisms for the conversion of GGPP **1** into tuberculosinol **3** and isotuberculosinol (nosyberkol) **4** through the intermediary tuberculosinyl diphosphate **2**. The Rv3377c enzyme is a Type B diterpene cyclase affording **2** from **1**.^{2,3} Peters group reported that the Rv3378c-encoded enzyme is a Type A cyclase to produce the tricyclic edaxadiene **5** from **2** (path *c*).⁹ However, our careful analysis^{4,6,7} demonstrated that the Rv3378c enzyme catalyzes the OPP-releasing reaction to afford the incipient C15-cation, to which a water molecule attacks to give **3** (path *a*), and the allylic migration concomitantly occurs to afford C13-cation, followed by the nucleophilic attack of a water molecule, leading to the production of **4** (path *b*). Very recently, the structure **5** was also revised to **4** by other workers who reported the chemical synthesis of **4**.^{10,11}

(*ent*-CDP, **8**), *syn*-copalyl diphosphate (*syn*-CDP, **9**), and halimane-type diphosphate (**2**), yielding sclarene (**13**), (*Z*)-biformene (**14**), and unnatural novel products of (4*aS*,5*R*,8*aS*)-1,1,4*a*-trimethyl-6-methylene-5-(3-methylenepent-4-enyl)decahydronaphthalene (**15**; named griseolaene) and halima-13(16), 14(15)-diene (**16**; named tuberculosene), respectively (Fig. 1).¹³ The conversion yields were *ca.* 50–60%.¹³ These findings indicate that the CYC2 enzyme is also classified as a new diterpene synthase that does not belong to diterpene cyclases and has great plasticity for various substrates.

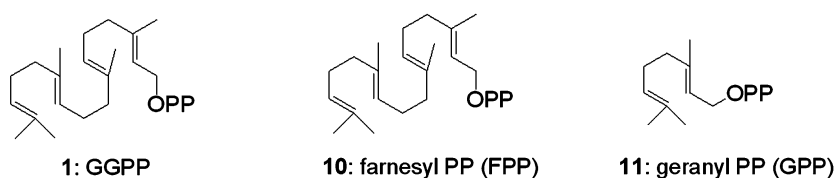
Next, we examined whether the Rv3378c enzyme also tolerates the bicyclic diterpene diphosphates **6–9**. These experiments allowed us to perform the first enzymatic synthesis of naturally occurring manool (**24**), *ent*-manool (**26**), and vitexifoin A (**28**); however, the acyclic terpenes **1**, **10**, and **11** were not

accepted as substrates. Therefore, the Rv3378c enzyme has broad substrate specificity like the CYC2 enzyme, although it is less plastic than CYC2. Interestingly, we have found that **3** and **4** inhibited the phagocytosis of opsonized zymosan particles by human macrophage-like cells. It is notable that the inhibitory activity was synergistically increased by the coexistence of **3** and **4b**. This biological activity was specifically found for **3** and **4**, but other bicyclic diterpenes (**13–16** and **23–28**) that we have created by enzymatic reactions had little or no inhibitory activity. These findings may imply that the production of **3** and **4** by the Rv3378c enzyme might be related to the virulence of *M. tuberculosis*. In this paper, we describe the substrate specificity of the Rv3378c enzyme and report the biological activities of **3**, **4**, and other labdane-related diterpenes against macrophage phagocytosis.

Bicyclic Substrates



Acyclic Substrates



Products by CYC2

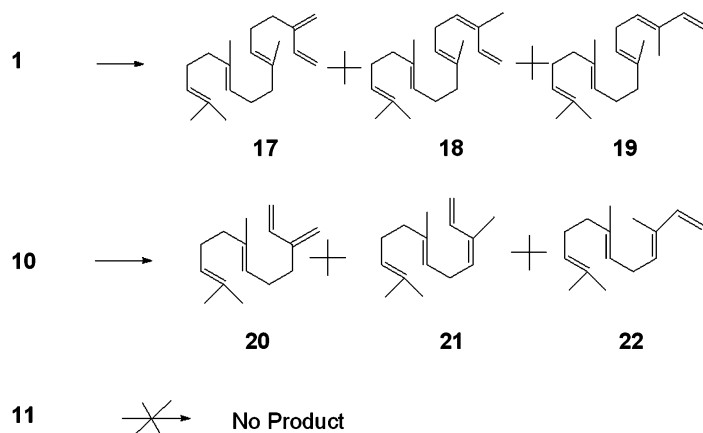
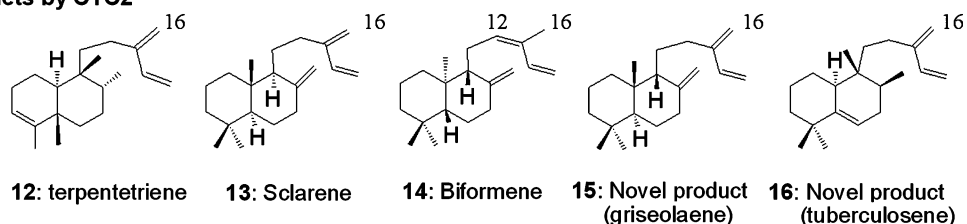


Fig. 1 Enzymatic products catalyzed by the CYC2 enzyme from *Kitasatospora griseola*. This enzyme catalyzes the formation of terpentetriene **11** from terpentedieryl diphosphate **6** as the original substrate.¹² However, the CYC2 enzymes exhibits the broad substrate specificity to accept the bicyclic diterpene diphosphates¹³ of CDP **6**, *ent*-CDP **7** and *syn*-CDP **8** and acyclic terpenes of GGPP **1** and FPP **10**,¹² but GPP **11** are not recognized.¹²

Results and Discussion

Substrate specificity of the Rv3378c enzyme

We checked the substrate specificity of the Rv3378c enzyme by using the bicyclic diterpene diphosphates **6–9**, which were enzymatically prepared in accordance with previous reports.^{12–16} The 3 CDP (**7–9**) synthases (N-terminal GST-fusion protein expressed by pGEX-4T-3 vector)^{14,15} and terpentedieryl-PP (**6**) synthase (called the CYC1 enzyme, N-terminal His₆-tagged protein expressed by pQE-30 vector)¹⁶ were expressed in *Escherichia*

coli BL21 (DE3); the cultures were grown in 2× YT medium and Luria–Bertani medium, respectively. Previously, we found that cell-free extracts obtained from *E. coli* cells exhibit phosphatase activity.^{2,3} To remove the endogenous phosphatase, each of the expressed proteins from 6-L cultures was purified by affinity column chromatography by using a glutathione-Sepharose 4B or Ni-NTA column. Optimal temperatures for the synthases of (-)-*ent*-CDP **17** and *syn*-CDP,¹⁷ and the CYC1 enzyme,¹² were reported to be around 30 °C and that for (+)-CDP synthase was reported to be 25 °C.¹⁴ At an approximately neutral pH range of 6–7.5, high activities were observed for the above 4 cyclases. On the other

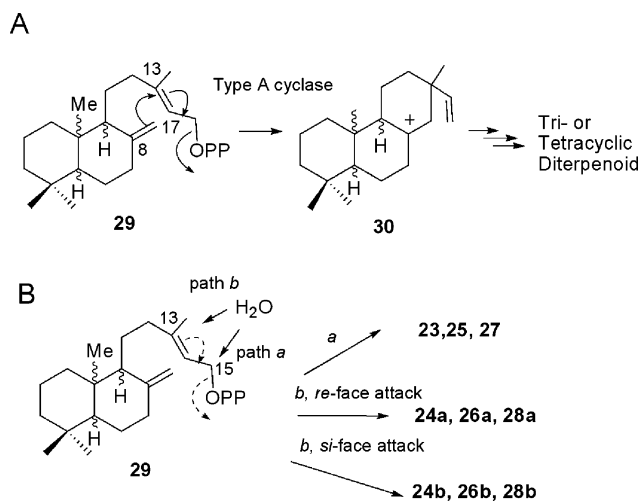
hand, the optimal temperature and pH for the Rv3378c enzyme were 45 °C and 7.0 (active at a pH range of 5.5–9.0), respectively.⁴ The divalent metal ion Mg²⁺ is essential for the enzymatic activities of all diterpene cyclases, including the Rv3378c enzyme. GGPP (**1**) was incubated under the following conditions to prepare **6–9**: **1** (3 mg, 50 μM), MgCl₂ (1 mM), DTT (2 mM), each of the purified cyclase enzymes from the 6-L culture, Tris-HCl buffer (pH 7.5, 50 mM) containing 0.1% Triton X-100 (total volume, 150 mL), 30 °C for 15 h. The reaction mixtures were then treated with acid phosphatase. The lipophilic materials were extracted with hexane, and then the hexane extracts were subjected to GC analyses. The peaks of (+)-copalol,¹⁸ (–)-*ent*-copalol,¹⁸ and *syn*-copalol¹⁹ were detected by GC analyses of each incubation mixture, and their structures were determined by comparing the resulting NMR data with those in the literature^{18,19} (see ESI, Fig. S1–S4† for the EIMS and detailed NMR analyses including DEPTs, ¹H–¹H COSY, NOESY, HMQC, and HMBC, measured in C₆D₆). However, no geranylgeraniol was detected by GC analyses of the hexane extracts from each of the incubation mixtures, demonstrating that the cyclization reactions for the formation of **6–9** had completed in the absence of **1** in the incubation mixture.

Next, we examined whether **6–9** were accepted as substrates of the Rv3378c enzyme. Each of these purified diterpene cyclases was mixed separately with the purified Rv3378c enzyme (13.7 μM), and the samples were incubated at 30 °C. At an incubation temperature of 45 °C (optimal temperature for the Rv3378c enzyme), bicyclic products were hardly detected; this was possibly due to the deactivation of all the cyclase enzymes (the CDP synthases and the CYC1 enzyme). The enzymatic reactions were terminated by adding 15% KOH/MeOH, followed by extraction of the enzymatic products with hexane. The hexane extracts, from which Triton X-100 was removed with a short SiO₂ column eluting with hexane:EtOAc (100:30), were subjected to GC analyses (ESI, Fig. S5†). No enzymatic product was detected from the incubation mixture of **6** (Fig. S5A), but the 3 CDPs (**7–9**) were converted by this enzyme (Fig. S5B–D†). These figures show that two enzymatic products were produced from each of the incubation reactions. All enzymatic products were purified through SiO₂ column chromatography eluting with hexane:EtOAc (100:0–100:5) and then subjected to NMR and MS analyses (ESI, Figs. S1–S4 and S6–S9†). Products **23** and **25** were assigned to be (+)-copalol and (–)-*ent*-copalol, respectively; $[\alpha]_D^{24} = +31$ (*c* 0.12, CHCl₃) for **23** (lit.¹⁸ $[\alpha]_D^{24} = +31.2$ (*c* 1.14, CHCl₃)) and $[\alpha]_D^{22} = -30$ (*c* 0.11, CHCl₃) for **25** (lit.¹⁸ $[\alpha]_D^{22} = -35.5$ (*c* 1.14, CHCl₃)). Product **27** was determined to be *syn*-copalol: $[\alpha]_D^{24} = +16.2$ (*c* 0.17, CHCl₃) for **27** (lit.¹⁹ $[\alpha]_D^{24} = +17.7$ (*c* 2.39, CHCl₃)). Products **23**, **25**, and **27** were not produced in the absence of the Rv3378c enzyme. Furthermore, treatment of **7–9** with 15% KOH/MeOH did not produce **23**, **25** and **27**. Thus, compounds **23**, **25**, and **27** that were produced are not chemical artifacts but true enzymatic products. As shown in Fig. S5 (ESI†), other products, **24**, **26**, and **28**, besides **23**, **25**, and **27** were found and were subjected to detailed NMR analyses, including 2D NMR. In addition to the bicyclic cores, **24**, **26**, and **28** all had a vinyl group in the side chain. For product **28**, the following ¹H-NMR data were found: H_b-15 (1H, δ_H 5.06, dd; $J_{Hb15-H14} = 10.8$ Hz, $J_{Ha15-Hb15} = 1.6$ Hz), H_a-15 (1H, δ_H 5.31, dd; $J_{Ha15-H14} = 17.2$ Hz, $J_{Ha15-Hb15} = 1.4$ Hz) and H-14 (1H, δ_H 5.89, dd; $J_{Ha15-H14} = 17.2$ Hz, $J_{Hb15-H14} = 10.8$ Hz). The chemical shift of C-13 was found at 72.91 ppm (s), indicating that the tertiary

alcohol group is positioned at C-13. In addition, the following HMBC cross peaks were found: Me-16/C-12, Me-16/C-13, and Me-16/C-14. Therefore, a moiety of 3-methylpent-1-en-3-ol was connected to the bicyclic skeleton. The above-mentioned NMR data were also observed for **24** and **26**. Therefore, **24**, **26**, and **28** were determined to be manool,^{20–22} *ent*-manool,^{23–25} and vitexifolin A,²⁶ respectively (ESI, Figs. S6–S10†). Fig. S11 in ESI† depicts the ¹H NMR spectra of product **24** (A), the authentic (13*R*)-manool **24a** (B), and product **26** (C). Comparison of Figs. S11A† with S11B† shows that the enzymatic product **24** involved both 13*R*-manool (**24a**) and 13*S*-manool (**24b**). This was further supported by the analysis in a GC-MS equipped with a chiral GC column (Fig. 3A). Product **24** was separated into 2 peaks. The first peak corresponded to authentic 13*R*-manool (**24a**) (Fig. 3B); thus, the second peak was assigned to be (13*S*)-manool (**24b**). The EIMS spectrum of **24a**, including the fragment pattern, was identical to that of **24b**. The ratio of **24a** to **24b** was 1:1.20 (Fig. 3A). The chemical shifts of some carbons in the ¹³C NMR spectra were slightly different between **24a** and **24b**, which was described in ESI (Figs. S6 and S7†). The chemical shifts (δ_C, ppm) of **24b** were assigned by comparing with those of the authentic **24a**. In the case of the ¹H NMR spectrum of the isolated **26** (ESI, Fig. S11C†), the larger signals of H-14, Ha-15, Hb-15, H-17, Me-16, and Me-20 were accompanied by the smaller peaks of the corresponding protons (*ca.* 1/5-fold intensity), and the spin–spin coupling patterns of these small peaks were the same as those of the large peaks. This finding suggests that two stereoisomers were mixed in a *ca.* 1:5 ratio, which was further confirmed by analysis in a GC-MS fitted with a chiral column (Fig. 3C). We could not obtain authentic 13*R-ent*-manool (**26a**) or 13*S-ent*-manool (**26b**); therefore, we intended to assign the stereochemistries of **26a** and **26b** by detailed NMR analyses. The ¹H NMR spectrum of the major peak (ESI, Fig. S11C†) was completely identical to that of the authentic 13*R*-manool (**24a**) (Fig. S11B†). This finding demonstrates that the major (second) peak corresponded to 13*S-ent*-manool (**26b**), but not to 13*R-ent*-manool (**26a**) because (–)-**26b** is an enantiomeric counterpart of (+)-**24a**. Therefore, the smaller (first) peak on the chiral GC-MS (Fig. 3C) was determined to be *ent*-13*R*-manool (**26a**), which was further supported by the finding that the ¹H NMR spectra of **26a** and **24b** were identical. Assignment of the smaller peak (Fig. S11C†) to **26a** (13*R*-configuration) was further validated by comparing the ¹H NMR data (CDCl₃) of **26a** with the published NMR data of *ent*-13*R*-manool **24a** measured in CDCl₃.^{24,25} The chemical shift differences were minimal between them (ESI, Fig. S12 and Table S1†). From Fig. 3C, the product ratio of the 13*R*- (**26a**) and 13*S*- (**26b**) isomers was estimated to be *ca.* 1:5. We can surmise with high credibility that the first peak on the chiral column is allocated to be the 13*R*-isomer, while the second peak can be assigned to the 13*S*-isomer, given that both stereoisomers consist of identical bicyclic skeleton. Product **28** was also separable on the chiral GC column (Fig. 3D); it is inferable that the first peak is the 13*R*-isomer, while the second peak is the 13*S*-isomer. Thus, the product ratio of **28a** to **28b** was determined to be 1:17 (Fig. 3D and ESI, Fig. S13†). Vitexifolin A, isolated from *Vitex rotundifolia*,²⁶ was subjected to analysis in a GC-MS equipped with a chiral column (Fig. 3E) and to ¹H-NMR analysis (ESI, Fig. S13†). Fig. 3E shows that the stereochemistry of natural vitexifolin A was exclusively the 13*R* configuration, but a negligible amount of the 13*S*-form was mixed

in the natural diterpene (see ESI, Fig. S13†). The stereochemistry of the main enzymatic product vitexifolin A (13*S*) was opposite to that of the natural one (13*R*). This is the first report on the enzymatic synthesis of the diterpenoids manool, *ent*-manool, and vitexifolin A.

Following the reaction mechanism shown in Scheme 1, substrates **7**, **8**, and **9** were converted to **23**, **25**, and **27**, respectively, *via* path *a*. On the other hand, these substrates were transformed into **24ab**, **26ab**, and **28ab**, respectively, *via* path *b* (see also Scheme 2B). Production of **23–28** further verified that the Rv3378c enzyme is not a type A cyclase, but catalyzes the removal reaction of OPP moiety, followed by addition of water to the generated cation, resulting in the production of diterpene alcohols **23–28**. The substrate specificity was remarkably broad; the 3 labdane-type CDPs **7–9** were accepted as substrates of Rv3378c, with high yields (isolation yields 67–78%). However, no enzymatic product was detected from the incubation mixture of **6** with the Rv3378c protein, indicating that clerodane skeleton **6** could not be accepted as a substrate. Following Fig. 3 and Fig. S5 (ESI†), in conjunction with the isolation yields of each of diterpenes **23–28**, the product distributions were calculated as shown in the parentheses of Fig. 2. When *ent*-CDP **8** was used instead of CDP **7**, the direction of path *a* was suppressed and the production of 13*S*-isomer **26b** was more increased than 13*R*-isomer **26a**. This product diastereoselectivity indicates that the Rv3378c enzyme somewhat distinguishes the enantiomers CDP and *ent*-CDP inside the reaction cavity. In addition, path *a* for **9** was more significantly suppressed compared with that for **7**; in turn, path *b* became enhanced to give a higher yield of **28** than that of **27**. Furthermore,



Scheme 2 Enzymatic reaction mechanisms by diterpene synthases. The three CDPs of CDP **7**, *ent*-CDP **8** and *syn*-CDP **9** are represented by **29**. (A) Type A diterpene cyclases mediate the formation of cation **30** from **29**. Cation **30** is frequently encountered in the biosyntheses of *ent*-kaurene, *ent*-cassa-12,15-diene, *ent*-sandaraco-pimaradiene, *syn*-pimara-7,15-diene, *syn*-stemar-13-ene, and so on.^{34–37} (B) Enzymatic reaction mechanism of **29** by the Rv3378c gene product to afford **23–28**.

the higher diastereoselectivity was generated to afford a higher production of **28b** than that of **28a**. The CYC2 enzyme from *K. griseola* is able to accept acyclic diphosphates of GGPP (**1**) and FPP (**9**), but is inactive to GPP (**10**) (Fig. 1).¹² On the other hand, the Rv3378c enzyme failed to recognize all of the acyclic terpenes

Products by Rv3378c

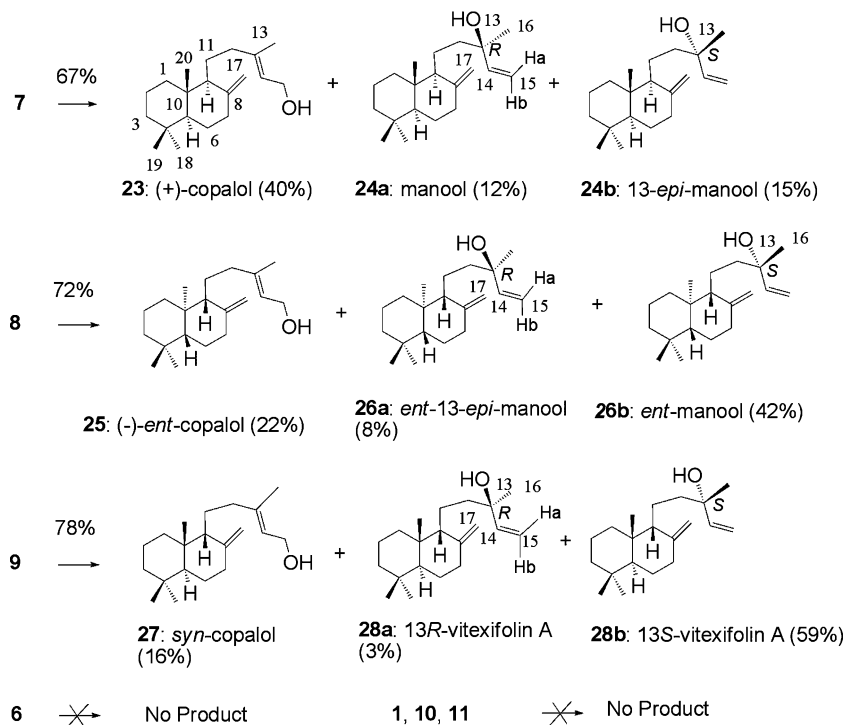


Fig. 2 Enzymatic products **23–28** produced by the catalytic action of the Rv3378c enzyme. This enzyme accepts bicyclic diphosphates **7–9**, but fails to recognize **6** and acyclic terpenes of GPP **11**, FPP **10** and GGPP **1**.

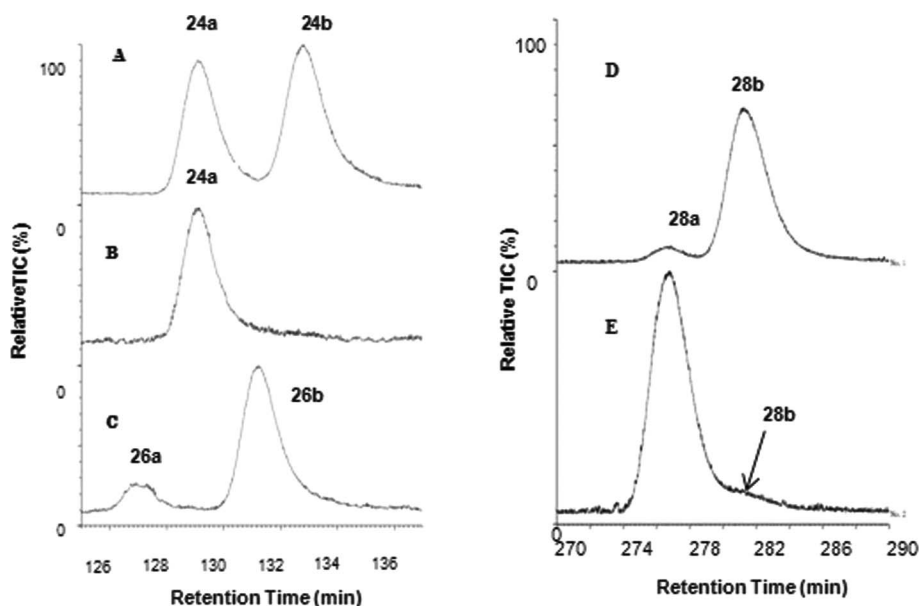


Fig. 3 GC-MS trace of product **24** (A), authentic (13*R*)-manool **24a** (B), product **26** (C), product **28** (D) and vitexifolin A (E) gifted by Prof. Ono.²⁶ The chromatograms were obtained by using a chiral column. Samples A, C and D are a mixture of 13*R*- and 13*S*-isomers, which were obtained by the enzymatic reactions with Rv3378c enzyme. Measurement condition: CYCLOSILB capillary column (0.32 mm × 30 m) (Agilent technologies); injection temp., 250 °C; initial temp., 140 °C; increased rate of temp., 0.01 °C min⁻¹. The GC-MS condition of (D) and (E) was the same as those of (A)–(C), but the initial temperature (120 °C) was different from that (140 °C) of (A)–(C).

1, **10**, and **11**. Thus, the Rv3378c enzyme has higher substrate specificity compared to the CYC2 enzyme.

Biological activity against macrophage phagocytosis

As described above, the *Rv3377c* and *Rv3378c* genes are found in virulent *Mycobacterium* species but not in avirulent ones.^{2–4} The enzymatic products **3** and **4** were tested to determine if they have a biological activity. Russell and coworkers reported that the survival of *M. tuberculosis* in the macrophage was attenuated by the disruption of the *Rv3377c* or *Rv3378c* gene through the insertion of a transposon,²⁷ suggesting that the two genes may be closely related to the pathogenicity of the organism. We have noted the antiphagocytic activity of **3** and **4**. We evaluated the effect of **3** and **4** on the phagocytic activity against zymosan, a yeast cell wall component that induces inflammatory responses, using human macrophage-like U-937 cells. None of the diterpenes used in this experiment, including **3** and **4**, affected the viability of cells (93–97%) at 0.1–20 μM. Fluorescence microscopic analysis revealed that the phagocytosis of opsonized zymosan particles (FITC-OPZ) by human macrophage-like U-937 cells treated with 10 μM of **3** was reduced to a level of 56% compared to untreated cells (Fig. 4). The Rv3378c-encoded enzyme produces both **3** and **4** in a ratio of 1:1.^{4,6,7} Compound **4** (a mixture of **4a** and **4b** in a ratio of 1:3)⁴ also exhibited the inhibitory effect to a level of ca. 65%. Surprisingly, the coexistence of **3** and **4** (10 μM each; total concentration 20 μM) synergistically inhibited the phagocytic action to the level of about 31% (Fig. 4). As described below, this synergistic observation was also found in a mixture of **3** and purified **4b** (10 μM each, total concentration 20 μM), without affecting the cell viability (see Fig. 5; compare the activities of 20 μM concentration for **3** and **3 + 4b**; also see ESI, Fig. S15†). On

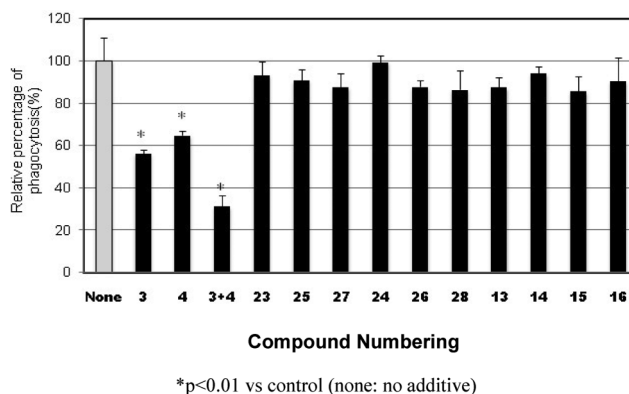
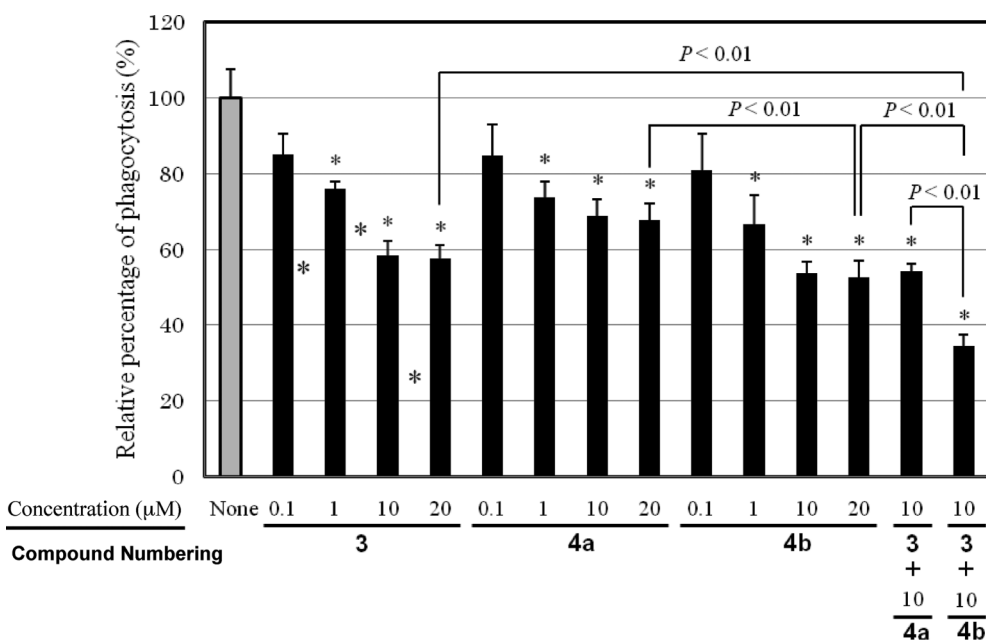


Fig. 4 Inhibition effects of diterpenes (**3**, **4**, **13–16** and **23–28**) against the phagocytosis of FITC-OPZ by macrophage-like U937 cells. The cells were treated with 10 μM each of diterpenes for 15 min and exposed to FITC-OPZ for 60 min at 37 °C. The biological activities of **4** and **24**, **26** and **28** were evaluated by using a mixture of 13*R*- and 13*S*-isomers, which was obtained by purifying with a SiO₂ column, but not with a chiral HPLC column, thereby the diastereomeric mixtures were included with the ratio of 13*R*- and 13*S*-isomers shown in the parentheses of Fig. 2. The cells engulfing FITC-OPZ were counted by fluorescence microscopy. The data are normalized using the value of untreated cells (Control) as 100% and expressed as mean ± SD (n = 3–5). * *P* < 0.01 vs. control (Student's *t*-test). In the case of **3 + 4**, a mixture of **3** and **4** (1:1; 10 μM each; total concentration: 20 μM) was used for this experiment, where **4** contained **4a** and **4b** in a ratio of 1:3.⁴

the other hand, diterpenes **13–16**¹³ and **23–28** had little effect, with no statistical significance (Fig. 4). Therefore, only **3** and **4** with the halimane skeleton had an inhibitory effect on phagocytosis among all the diterpenes tested in this experiment; however, **16** with a



*p<0.01 vs control (none: no additive)

Fig. 5 Inhibition activities of **3**, **4a** and **4b** against the phagocytosis of FITC-OPZ by macrophage-like U937 cells. The cells were treated with **3**, and/or **4a**, **4b** at 0.1 to 20 μM for 15 min and exposed to FITC-OPZ for 60 min at 37 °C. Concentration dependency vs. phagocytosis (%) was clearly observed with $R^2 = 0.96-0.98$ for **3**, **4a** and **4b** (see ESI, Fig. S12†). Comparison of the activities between **4a** and **4b** indicates that the activity of **4b** was higher than that of **4a**. Addition of **4b** to **3** conferred a remarkable synergistic effect. However, addition of **4a** to **3** exhibited little synergy, because the phagocytosis activity of (**3** + **4a**) was nearly the same as that of **3** at the same concentration of 20 μM. The cells engulfing FITC-OPZ were counted by fluorescence microscopy. The data are normalized using the value of untreated cells (control) as 100% and expressed as mean ± SD (n = 4). * $P < 0.01$ vs. control (Student's *t*-test).

halimane core had little or no effect on phagocytosis (Fig. 4). This finding demonstrates that the halimane scaffold involving the hydroxyl group either at C(13) or C(15) is essential for this activity. Fig. 5 shows a comparison of the inhibitory effect of **4a** with that of **4b**. Good correlations ($R^2 = 0.96-0.98$) were observed between the phagocytic percentages of the cells and the logarithmic concentrations (0.1–20 μM) of **4a** and **4b** (ESI, Fig. S14†). The activity of **4b** was higher than that of **4a** at any concentration (Fig. 5 and Fig. S15 in ESI†). Furthermore, the activity (ca. 30%) of **3** + **4b** was significantly higher compared to that (ca. 54%) of **3** + **4a**. When the inhibitory percentage of **3** + **4a** was compared with that (ca. 56%) of **3**, no marked enhancement in inhibition was observed (Fig. 5; compare the activities at the concentrations of 20 μM for **3**, **4a**, and **3** + **4a**; see also Fig. S15 in ESI†). This finding indicates that **4a** did show a synergistic action. Compound **2** (the diphosphate of **3**) had little activity at a concentration of 10 μM (data not shown), indicating that the release of the PP moiety is essential for this activity. Previously, we reported that the flanking gene *Rv3376* encodes the phosphatase that hydrolyzes the PP moiety of **2** to yield **3**.⁴ The *Rv3378c* and *Rv3376* enzymes may synergistically promote a higher production of **3**, thus leading to the enhanced inhibition of phagocytosis. Mann *et al.*⁹ have reported that edaxadine (**5**) inhibits phagosomal maturation, resulting in attenuated acidification and less active proteolysis. The structure of edaxadiene (**5**) proposed by Mann *et al.* was revised to that of isotuberculosinol (**4**).^{4,10,11} Thus, the antiphagocytic activity of **4** was clearly demonstrated by us and other researchers.^{9,27}

However, Mann *et al.* have never reported the inhibitory effect of **3** on phagocytosis.⁹ As shown in Scheme 1, the *Rv3378c* enzyme actually affords both **3** and **4**, with a higher production of **4b** than that of **4a** (ca. 3:1).⁴ This strong synergistic action of **3** and **4b** may cause the pathogenicity of *M. tuberculosis*. Although the molecular mechanisms by which virulent *Mycobacterium* species successfully survive and replicate within phagocytes are still unknown, previous studies by other researchers²⁸⁻³¹ have suggested that macrophages infected with pathogenic mycobacteria show decreased cell signalling and functions associated with microbicidal mechanisms. The present finding might suggest that virulent *M. tuberculosis* species residing in phagocytes attenuate phagocytic activity via their production of **3** and **4**. The *Rv3377c* and *Rv3378c* gene products for producing **3** and **4** might have been incorporated into virulent *Mycobacterium* species to interfere with intracellular signalling in phagocytes, resulting in impaired cell functions. Further biochemical investigations are necessary to clarify the detailed mechanism of this phenomenon.

Conclusion

We examined whether **3** and **4** can be detected from cultured cells of avirulent *Mycobacterium* species: 12 species were investigated, but neither compound was found in any of them.³² In addition, *Rv3377c* and *Rv3378c* genes are found only in virulent *Mycobacterium* species. Thus, both genes are likely to be related to the pathogenicity of the organism, which was further supported by the

finding of the inhibitory effect of **3** and **4** against the phagocytosis of opsonized zymosan particles by human macrophage-like cells. This interesting activity is found only in the halimane-type diterpenes involving the hydroxyl group at C-13 or C-15. The labdane-related diterpenes were found to have little activity. The strong synergistic inhibition was found in the presence of **3** and **4b**. This may further impair phagocyte function, which might contribute to the pathogenicity of *M. tuberculosis*. Thus, both enzymes are likely to be new potential targets in the development of new drugs. The Rv3378c-encoded enzyme showed markedly broad substrate specificity. The bicyclic diterpenoid diphosphates **7–9** were converted into **23–28**, with good yields. Scheme 2A shows that 3 bicyclic CDPs (**7–9**), represented by **29**, usually undergo further cyclization reaction to form **30** by a Type A cyclase, leading to tri- or tetracyclic skeleton,³³ as found in the biosynthesis of the carbocycles of pimaraene, abietane, cassane, kaurane, beyerane, stemarane, *etc.*^{34–37} The more extended ring-forming reactions occur due to the facile nucleophilic attack of the double bond at the C8-C17 to the C13 cation generated by the OPP-releasing reaction (Type A cyclase). However, neither the tricyclic nor the tetracyclic product was produced in the present experiments.

Instead, a water molecule attacked the carbocation generated after the release of diphosphate, resulting in the production of **23–28** (Scheme 2B). Thus, the Rv3378c enzyme is categorized to be a new diterpene synthase. The CYC2 enzyme from *K. griseola* also does not belong to the Type A cyclases.^{12,13,16} At present, no homologous gene to *cyc2* and *Rv3378c* has been reported. By using the CYC2 and Rv3378c enzymes, we succeeded in the first enzymatic synthesis of natural products **13**, **14**, **24**, **26**, and **28**, suggesting that some genes homologous to *cyc2* and *Rv3378c* exist in nature. Further isolation of the genes homologous to *cyc2* and *Rv3378c* from various biological sources may lead to the proposal of a new type of diterpene synthases.

Experimental Section

Analytical Method

NMR spectra of the enzymic product were recorded in C₆D₆ on a Bruker DMX 600 and DPX 400 spectrometers, the chemical shifts being given in ppm relative to the solvent peak $\delta_{\text{H}} = 7.28$ and $\delta_{\text{C}} = 128.0$ ppm as the internal reference for ¹H- and ¹³C NMR spectra, respectively. In the CDCl₃ solution, the chemical shifts are given in ppm relative to the solvent peak ($\delta_{\text{H}} = 7.26$ and $\delta_{\text{C}} = 77.0$ ppm). The coupling constants *J* are given in Hz. GC analyses were done on a Shimadzu GC-8A chromatograph equipped with a flame ionization detector (a DB-1 capillary column, 30 m × 0.25 mm × 0.25 μm, J&W Scientific, Inc.). GC-MS spectra were on a JEOL SX 100 or a JEOL JMS-Q1000 GC K9 instrument equipped with a ZB-5ms capillary column (30 m × 0.25 mm × 0.25 μm; Zebron) by using the EI mode operated at 70 eV. HR-EIMS was performed by direct inlet system. HPLC was carried out with Hitachi L-1700 (pump) and L-7405 (UV detector), the HPLC peaks having been monitored at 210 or 214 nm. Specific rotation values were measured with a Horiba SEPA-300 polarimeter. Chiral GC columns used to separate the stereoisomers were CYCLOSILB capillary column (0.32 mm × 30 m, Aligent technologies).

Incubation conditions of GGPP (**1**) with CDP synthases and Rv3378c enzymes

The diterpene cyclases of three CDP (CDP, *ent*-CDP and *syn*-CDP) were expressed as GST-fusion proteins in *E. coli* BL21 (DE3).^{14,15} The expressed proteins were purified by glutathione-Sepharose 4B, by which the endogenous phosphatase was removed and no hydrolysis of diphosphate group of **1** occurred. Each of the purified three CDP synthases from 6-L culture of *E. coli* and the purified Rv3378c enzyme from 6-L culture of *E. coli* were mixed. GGPP **1** (3 mg), 1 mM MgCl₂, 2 mM DTT and 0.1% TritonX-100 were dissolved in 50 mM Tris-HCl buffer (pH 7.5). Incubation (total volume: 150 ml) was done at 30 °C for 15 h. The enzymatic reaction was quenched by adding 15% KOH/MeOH, followed by heating 80 °C for 20 min. The enzymatic products were extracted with hexane, followed by SiO₂ column chromatography with hexane:EtOAc (100:0–100:5), yielding the pure enzymatic products **23–28**. The conversions of **1** to the three CDPs **7–9** were complete under the aforementioned conditions, because no GGOH was recovered from the incubation mixture of **1** with the three CDP synthases after the treatment with phosphatase.

Spectroscopic data of **23**, **24a**, **24b**, **25**, **26a**, **26b**, **27**, **28a** and **28b**

Products 23, 25 and 27. ¹H- and ¹³C NMR data of **23**, **25** and **27** are described in ESI (Figs. S2–S4†). The EIMS are depicted in Fig. S2 (ESI). The values of specific rotations $[\alpha]_{\text{D}}$ are given in the text.

Products 24a and 24b. The chemical shifts of **24a** and **24b** were separable (ESI, Figs. S6, S7 and S11†). Authentic **24a** was purchased from Industrial Research Limited (New Zealand).

24a: ¹H NMR (400 MHz, C₆D₆): δ 0.857 (Me-20, 3H, s), 0.916 (Me-19, 3H, s), 0.973 (Me-18, 3H, s), 1.05 (H-1, m), 1.10 (H-5, bd, *J* = 12.4 Hz), 1.257 (Me-16, 3H, s), 1.26 (H-3, m), 1.40 (2H, H-6 & H-12, m), 1.48 (H-3, m), 1.54 (H-2, m), 1.59 (H-11, m), 1.62 (H-9, m), 1.65 (H-2, m), 1.74 (H-11, m), 1.75 (H-6, m), 1.84 (H-1, m), 1.88 (H-12, m), 2.08 (H-7, ddd, *J* = 12.8, 12.8, 4.8 Hz), 2.51 (H-7, bd, *J* = 12.8 Hz), 4.83 (H-17, bs), 5.08 (H-17, bs), 5.10 (Hb-15, dd, *J* = 10.8, 1.6 Hz), 5.34 (Ha-15, dd, *J* = 17.2, 1.6 Hz), 5.94 (H-14, dd, *J* = 17.2, 10.8 Hz); ¹³C NMR (100 MHz, C₆D₆): δ 14.68 (C-20, q), 18.01 (C-11, t), 19.73 (C-2, t), 21.88 (C-19, q), 24.71 (C-6, t), 28.53 (C-16, q), 33.64 (C-4, s), 33.74 (C-18, q), 38.70 (C-7, t), 39.22 (C-1, t), 40.08 (C-10, s), 41.74 (C-12, t), 42.45 (C-3, t), 55.65 (C-5, d), 57.48 (C-9, d), 73.24 (C-13, s), 106.9 (C-17, t), 111.4 (C-15, t), 145.7 (C-14, d), 148.8 (C-8, s).

24b: ¹H NMR (400 MHz, C₆D₆): δ 0.857 (Me-20, 3H, s), 0.916 (Me-19, 3H, s), 0.973 (Me-18, 3H, s), 1.05 (H-1, m), 1.10 (H-5, bd, *J* = 12.4 Hz), 1.26 (H-3, m), 1.264 (Me-16, 3H, s), 1.38 (H-12, m), 1.40 (H-6, m), 1.48 (H-3, m), 1.54 (H-2, m), 1.59 (H-11, m), 1.62 (H-9, m), 1.65 (H-2, m), 1.74 (H-11, m), 1.75 (H-6, m), 1.84 (H-1, m), 1.90 (H-12, m), 2.08 (H-7, ddd, *J* = 12.8, 12.8, 4.8 Hz), 2.51 (H-7, bd, *J* = 12.8 Hz), 4.88 (H-17, s), 5.08 (H-17, s), 5.09 (Hb-15, dd, *J* = 10.8, 1.6 Hz), 5.32 (Ha-15, dd, *J* = 17.2, 1.6 Hz), 5.93 (H-14, dd, *J* = 17.2, 10.8 Hz); ¹³C NMR (100 MHz, C₆D₆): δ 14.68 (C-20, q), 18.07 (C-11, t), 19.75 (C-2, t), 21.88 (C-19, q), 24.71 (C-6, t), 28.22 (C-16, q), 33.64 (C-4, s), 33.74 (C-18, q), 38.70 (C-7, t), 39.23 (C-1, t), 40.09 (C-10, s), 41.80 (C-12, t), 42.45 (C-3, t), 55.68 (C-5, d), 57.53 (C-9, d), 73.14 (C-13, s), 107.1 (C-17, t), 111.2 (C-15, t), 145.9 (C-14, d), 148.7 (C-8, s).

24 (a mixture of **24a** and **24b**): EIMS (%) m/z 81 (100), 95 (70), 137 (72), 257 (48), 290 (M^+ , 0.4). HRMS (EI) m/z found 290.2605 (M^+ , $C_{20}H_{34}O$ requires 290.2610). $[\alpha]_D^{24} + 31.5$ (c 0.08, $CHCl_3$), *cf. lit.*^{20,21} $[\alpha]_D^{24} + 28.0$ (c 1.5, $CHCl_3$)²¹ for **24a** $[\alpha]_D^{24} + 46.4$ (c 0.7, $CHCl_3$)²⁰ for **24b** and $[\alpha]_D^{24} + 26.9$ (c 0.05, $CHCl_3$) for the commercially available **24a**.

Products 26a and 26b. NMR data of the major product **26b**: 1H NMR (400 MHz, C_6D_6): δ 0.857 (Me-20, 3H, s), 0.915 (Me-19, 3H, s), 0.971 (Me-18, 3H, s), 1.03 (H-1, m), 1.10 (H-5, bd, $J = 12.4$ Hz), 1.25 (H-3, m), 1.256 (Me-16, 3H, s), 1.39 (H-6, m), 1.40 (H-12, m), 1.47 (H-3, m), 1.55 (H-11, m), 1.56 (H-2, m), 1.62 (H-9, m), 1.65 (H-2, m), 1.73 (H-11, m), 1.75 (H-6, m), 1.84 (H-1, m), 1.85 (H-12, m), 2.08 (H-7, ddd, $J = 12.8, 12.8, 4.8$ Hz), 2.51 (H-7, bd, $J = 12.8$ Hz), 4.83 (H-17, bs), 5.07 (H-17, bs), 5.10 (Hb-15, dd, $J = 10.8, 1.6$ Hz), 5.34 (Ha-15, dd, $J = 17.2, 1.6$ Hz), 5.94 (H-14, dd, $J = 17.2, 10.8$ Hz); ^{13}C NMR (100 MHz, C_6D_6) δ 14.68 (C-20, q), 18.02 (C-11, t), 19.74 (C-2, t), 21.89 (C-19, q), 24.74 (C-6, t), 28.54 (C-16, q), 33.65 (C-4, s), 33.75 (C-18, q), 38.70 (C-7, t), 39.22 (C-1, t), 40.08 (C-10, s), 41.74 (C-12, t), 42.45 (C-3, t), 55.66 (C-5, d), 57.49 (C-9, d), 73.25 (C-13, s), 106.9 (C-17, t), 111.4 (C-15, t), 145.8 (C-14, d), 148.8 (C-8, s).

The minor product **26a**: the 1H NMR data (600 MHz, $CDCl_3$) are given in ESI (Fig. S12[†]), comparing with that of **26b**. The ^{13}C NMR data were not collected due to the small amount of **26a** involved in the mixture of **26a** and **26b**.

26 (a mixture of **26a** and **26b**): EIMS (%) m/z 81 (100), 95 (70), 137 (73), 257 (50), 290 (M^+ , 0.4). HRMS (EI) m/z found 290.2605 (M^+ , $C_{20}H_{34}O$ requires 290.2610). $[\alpha]_D^{20} -32.1$ (c 0.1, $CHCl_3$), *cf. lit.*²³ $[\alpha]_D^{20} -44.3$ ($CHCl_3$) for **26a** and $[\alpha]_D^{20} -29.5$ ($CHCl_3$) for **26b**.

Products 28a and 28b. NMR data of the minor product **28a**, which corresponds to the sample kindly gifted by Prof. Ono;²⁶ 1H NMR (400 MHz, C_6D_6): δ 0.928 (Me-18, 3H, s), 0.954 (Me-19, 3H, s), 1.124 (Me-20, 3H, s), 1.17 (H-1, m), 1.24 (H-3, m), 1.241 (Me-16, 3H, s), 1.34 (H-12, m), 1.42 (H-6, m), 1.46 (H-5, m), 1.47 (H-3, m), 1.54 (H-2, m), 1.63 (3H, H-9, H-11 & H-12, m), 1.65 (H-6, m), 1.75 (2H, H-1 & H-2, m), 1.83 (H-11, m), 2.25 (H-7, 2H, m), 4.74 (H-17, m), 4.93 (H-17, t, $J = 2.2$ Hz), 5.07 (Hb-15, dd, $J = 10.8, 1.6$ Hz), 5.31 (Ha-15, dd, $J = 17.2, 1.6$ Hz), 5.91 (H-14, dd, $J = 17.2, 10.8$ Hz); ^{13}C NMR (100 MHz, C_6D_6) δ 19.54 (C-2, t), 20.40 (C-11, t), 22.36 (C-18, q), 22.70 (C-20, q), 24.02 (C-6, t), 28.36 (C-16, q), 31.91 (C-7, t), 33.30 (C-4, s), 33.60 (C-19, q), 37.09 (C-1, t), 38.41 (C-10, s), 41.34 (C-12, t), 42.84 (C-3, t), 46.08 (C-5, d), 58.83 (C-9, d), 72.82 (C-13, s), 109.7 (C-17, t), 111.2 (C-15, t), 146.0 (C-14, d), 149.6 (C-8, s). NMR data of **28a** in $CDCl_3$ was reported in the ref. 26, but the 1H NMR spectra of **28a** and **28b** measured in C_6D_6 were more separable than those in $CDCl_3$.

NMR data of the major product **28b**: 1H NMR (400 MHz, C_6D_6): δ 0.927 (Me-18, 3H, s), 0.948 (Me-19, 3H, s), 1.124 (Me-20, 3H, s), 1.18 (H-1, m), 1.23 (H-3, m), 1.246 (Me-16, 3H, s), 1.35 (H-6, m), 1.37 (H-12, m), 1.45 (H-5, m), 1.46 (H-3, m), 1.52 (H-2, m), 1.60 (H-12, m), 1.61 (H-11, m), 1.62 (H-9, m), 1.63 (H-6, m), 1.75 (2H, H-1 & H-2, m), 1.87 (H-11, m), 2.26 (H-7, 2H, m), 4.75 (H-17, m), 4.93 (H-17, t, $J = 2.2$ Hz), 5.06 (Hb-15, dd, $J = 10.8, 1.6$ Hz), 5.31 (Ha-15, dd, $J = 17.2, 1.6$ Hz), 5.89 (H-14, dd, $J = 17.2, 10.8$ Hz); ^{13}C NMR (100 MHz, C_6D_6) δ 19.54 (C-2, t), 20.41 (C-11, t), 22.36 (C-18, q), 22.70 (C-20, q), 24.02 (C-6, t), 28.73 (C-16, q),

31.92 (C-7, t), 33.30 (C-4, s), 33.60 (C-19, q), 37.08 (C-1, t), 38.39 (C-10, s), 41.35 (C-12, t), 42.82 (C-3, t), 46.10 (C-5, d), 58.76 (C-9, d), 72.91 (C-13, s), 109.7 (C-17, t), 111.3 (C-15, t), 145.8 (C-14, d), 149.6 (C-8, s)

28 (a mixture of **28a** and **28b**): EIMS (%) m/z 81 (100), 95 (70), 137 (67), 257 (48), 290 (M^+ , 0.36). HRMS (EI) m/z found 290.2619 (M^+ , $C_{20}H_{34}O$ requires 290.2610). $[\alpha]_D^{19} + 13.8$ (c 0.13, acetone), *cf. lit.*²⁶ $[\alpha]_D^{19} + 5.2$ (acetone) for **28a**. In the ref. 26, the C(13)-configuration was not determined, but we could determine the stereochemistry to be 13*R*, based on the behavior of the chiral column for GC (see Fig. 3).

Phagocytosis assay

Human lymphoma U937 cells were obtained from Cell Resource Center for Biomedical Research, Institute of Development, Aging and Cancer, Tohoku University. U937 cells were induced to differentiate into macrophage-like cells upon cultivation with phorbol 12-myristate 13-acetate at 20 nM for 2 days. As a target for phagocytosis of macrophage-like cells, FITC-labeled opsonized zymosan (FITC-OPZ) was used (FITC: fluorescein isothiocyanate). 10 mg of zymosan (Sigma, St Louis, Mo., USA) was incubated with 1 mg ml⁻¹ FITC (Dojindo, Kumamoto, Japan) in 50 mM sodium carbonate solution (pH 9.5) for 10 min in the dark at room temperature, and for opsonization, the resultant FITC-labeled zymosan was incubated with with 50% human serum/Hanks' balanced salt solution (HBSS) at 37 °C for 45 min. Macrophage-like cells were treated with diterpenes including tuberculosinol and isotuberculosinol at 37 °C for 15 min, followed by adding FITC-OPZ at final concentration of 500 µg ml⁻¹ to the cell culture. After incubation at 37 °C for 60 min, phagocytosis was stopped by setting the cells on ice. The extracellular fluorescence caused by free FITC-OPZ was quenched by 4% trypan blue/HBSS for 5 min. Cells were then washed and fixed in 4% paraformaldehyde/HBSS at room temperature for 10 min. Three microscopic fields containing 100 to 150 cells each were counted for each sample, and the degree of phagocytosis was presented as a mean percentage of fluorescent cells. Compared to control (no addition of diterpenoids), no significant difference in cell viability, which was assessed by trypan blue dye exclusion test, was observed when the concentration of any diterpenes was increased up to 20 µM.

Acknowledgements

This work was supported in part by Grant-in-Aid given to T. H. for Scientific Research from the Ministry of Education, Culture, Sports, Science and Technology, Japan. We thank Dr T. Toyomasu (Yamagata University) for providing us the plasmids harboring the genes for CDP-, *ent*-CDP and *syn*-CDP synthases. Thanks are given to Professors T. Dairi (Hokkaido University), T. Sassa (Yamagata University) and Dr S. Seto (Hamamatsu University School of Medicine) for the valuable suggestion. Thanks are also given to Prof. Y. Asakawa and Dr F. Nagashima (Tokushima Bunri University) for kindly providing the NMR spectra of *ent*-13epi-manool. We appreciate Prof. M. Ono (Kyushu Tokai University) and Prof. M. Davies-Coleman (Rhodes University, South Africa) for the kind gift of vitexifolin A and manool, respectively.

References

- 1 K. Andries, P. Verhasselt, J. Guillemont, H. W. H. Göhlmann, J-M Neefs, H. Winkler, J. V. Gestel, P. Timmerman, M. Zhu, E. Lee, P. Williams, D. de Chaffoy, E. Huitric, S. Hoffner, E. Cambau, C. Truffot-Pernot, N. Lounis and V. Jarlier, *Science*, 2005, **307**, 223–227.
- 2 C. Nakano, T. Okamura, T. Sato, T. Dairi and T. Hoshino, *Chem. Commun.*, 2005, 1016–1018.
- 3 (a) C. Nakano and T. Hoshino, *ChemBioChem*, 2009, **10**, 2060–2071; (b) C. Nakano and T. Hoshino, *ChemBioChem*, 2009, **10**, 2413–2414, Erratum.
- 4 C. Nakano, T. Ootsuka, K. Takayama, T. Mitsui, T. Sato and T. Hoshino, *Biosci. Biotechnol. Biochem.*, 2011, **75**, 75–81.
- 5 F. M. Mann, S. Priscic, H. Hu, M. Xu, R. M. Coates and R. J. Peters, *J. Biol. Chem.*, 2009, **284**, 23574–23579.
- 6 C. Nakano, T. Sato and T. Hoshino, 49th *Koryo, Terupen oyobi Seiyu Kagaku ni kansuru Toronkai (Symposium on the Chemistry of Tepenes, Essential Oils, and Aromatics)*, Nov. (2005), Fukui, Japan. Abstract pp 247–249 (in Japanese). See: <http://sciencelinks.jp/j-east/article/200602/000020060205A1034816.php>.
- 7 C. Nakano, T. Okamura, T. Sato, T. Hara, T. Dairi, T. Toyomasu, T. Sassa and T. Hoshino, 48th *Temmen Yuukikagoubutu Toronkai (Symposium on the Chemistry of Natural Products)*, Oct. (2006), Sendai, Japan, Symposium paper, pp 19–24 (in Japanese). see: <http://ci.nii.ac.jp/naid/110006682624/en>.
- 8 A. Rudi, M. Akin, E. Gaydon and Y. Kashman, *J. Nat. Prod.*, 2004, **67**, 1932–1935.
- 9 F. M. Mann, M. Xu, X. Chen, D. B. Fulton, D. G. Russell and R. J. Peters, *J. Am. Chem. Soc.*, 2009, **131**, 17526–17527.
- 10 N. Maugel, F. M. Mann, M. L. Hillwig, R. J. Peters and B. B. Snider, *Org. Lett.*, 2010, **12**, 2626–2629.
- 11 J. E. Spangler, C. A. Carson and E. J. Sorensen, *Chem. Sci.*, 2010, **1**, 202–205.
- 12 Y. Hamano, T. Kuzuyama, N. Itoh, K. Furihata, H. Seto and T. Dairi, *J. Biol. Chem.*, 2002, **277**, 37098–37104.
- 13 C. Nakano, T. Hoshino, T. Sato, T. Toyomasu, T. Dairi and T. Sassa, *Tetrahedron Lett.*, 2010, **51**, 125–128.
- 14 T. Toyomasu, R. Niida, H. Kenmoku, Y. Kanno, S. Miura, C. Nakano, Y. Shiono, W. Mitsuhashi, H. Toshima, H. Oikawa, T. Hoshino, T. Dairi, N. Kato and T. Sassa, *Biosci., Biotechnol., Biochem.*, 2008, **72**, 1038–1047.
- 15 K. Otomo, H. Kenmoku, H. Oikawa, W. A. König, H. Toshima, W. Mitsuhashi, H. Yamane, T. Sassa and T. Toyomasu, *Plant J.*, 2004, **39**, 886–893.
- 16 T. Dairi, Y. Hamano, T. Kuzuyama, N. Itoh, K. Furihata and H. Seto, *J. Bacteriol.*, 2001, **183**, 6085–6094.
- 17 Y. Hayashi, T. Toyomasu, Y. Hirose, Y. Onodera, W. Mitsuhashi, H. Yamane, T. Sassa and T. Dairi, *Biosci., Biotechnol., Biochem.*, 2008, **72**, 523–530.
- 18 H. Toshima, H. Oikawa, T. Toyomasu and T. Sassa, *Tetrahedron*, 2000, **56**, 8443–8450.
- 19 N. K. N. Yee and R. M. Coates, *J. Org. Chem.*, 1992, **57**, 4598–4608.
- 20 A. F. Barrero, J. F. Sanchez, A. J. Alvarez-Manzaneda, M. M. Dorado and A. Haidour, *Phytochemistry*, 1993, **32**, 1261–1265.
- 21 J. Villamizar, T. Fuentes, F. Salazar, E. Tropper and R. Alonso, *J. Nat. Prod.*, 2003, **66**, 1623–1627.
- 22 K. Bruns, *Tetrahedron Lett.*, 1970, **11**(37), 3263–3264.
- 23 R. M. Dawson, I. M. Godfrey, R. W. Hogg and J. R. Knox, *Aust. J. Chem.*, 1989, **42**, 561–579.
- 24 F. Nagashima, H. Tanaka and Y. Asakawa, *Phytochemistry*, 1996, **42**, 93–96.
- 25 A. A. Urzua, E. Tojo and J. Soto, *Phytochemistry*, 1995, **38**, 555–556.
- 26 M. Ono, T. Yanaka, M. Yamamoto, Y. Ito and T. Nohara, *J. Nat. Prod.*, 2002, **65**, 537–541.
- 27 K. Pethe, D. L. Swenson, S. Alonso, J. Anderson, C. Wang and D. G. Russell, *Proc. Natl. Acad. Sci. U. S. A.*, 2004, **101**, 13642–13647.
- 28 Z. A. Malik and G. M. Denning, *J. Exp. Med.*, 2000, **191**, 287–302.
- 29 S. K. Roach and J. S. Schorey, *Infect. Immun.*, 2002, **70**, 3040–3052.
- 30 P. Mueller and J. Pieters, *Immunobiology*, 2006, **211**, 549–556.
- 31 J. Pieters, *Cell Host Microbe*, 2008, **3**, 399–407.
- 32 T. Sato, A. Kigawa, R. Takagi, T. Adachi and T. Hoshino, *Org. Biomol. Chem.*, 2008, **6**, 3788–3794.
- 33 D. W. Christianson, *Chem. Rev.*, 2006, **106**, 3412–3442.
- 34 J. MacMillan and M. H. Beale in *Isoprenoids including Carotenoids* D. Cane, ed. in *Comprehensive Natural Products Chemistry*, D. Barton, K. Nakanishi and O. Meth-Cohn, ed., Elsevier, Amsterdam, 1999, Vol. 2, pp.217–244.
- 35 T. Toyomasu, *Biosci., Biotechnol., Biochem.*, 2008, **72**, 1168–1175.
- 36 C. Ikeda, Y. Hayashi, N. Itoh, H. Seto and T. Dairi, *J. Biochem.*, 2007, **141**, 37–45.
- 37 M. Xu, R. Widerman and R. J. Peters, *Proc. Natl. Acad. Sci. USA*, 2007, **104**, 7397–7401.